arXiv:1402.5844v1 [cond-mat.mes-hall] 24 Feb 2014

Coplanar waveguide based ferromagnetic resonance in ultrathin film magnetic nanostructures: impact of conducting layers

H. Głowiński,[1] M. Schmidt,[1] I. Gościańska,[2] J. Dubowik,[1] and J-Ph. Ansermet[3]
[1)] *Institute of Molecular Physics, Polish Academy of Sciences, PL-60179 Poznań, Poland*
[2)] *Faculty of Physics, A.Mickiewicz University, Umultowska 85, PL-61614 Poznań, Poland*
[3)] *Institute of Condensed Matter Physics, Station 3, Ecole Polytechnique Fédérale de Lausanne EPFL, CH-1015 Lausanne, Switzerland*

(Dated: 25 February 2014)

We report broadband ferromagnetic resonance (FMR) measurements based on coplanar waveguide (CPW) in ultrathin film structures comprising in-plane/ out-of-plane decoupled magnetic layers, which are deposited on nonmagnetic buffer layers of various thickness or other structures resulting in diverse sheet resistivity. We show that the excitation of the fundamental mode can be substantially (up to 10 times) enhanced in the structures deposited on buffer layers with a low sheet resistance in comparison to the structures deposited on weakly conducting buffer layers. The results are analyzed in terms of shielding of the electromagnetic field of CPW by a highly conducting film. The effect of enhancement of FMR absorption may be attractive for applications in spintronic devices that utilize magnetization dynamics of ultrathin ferromagnetic layers.

PACS numbers: 76.50.+g, 75.40.Gb, 75.40.Mg

I. INTRODUCTION

Ferromagnetic resonance (FMR) based on a vector network analyzer (VNA) and a coplanar waveguide (CPW) has become a common experimental tool for studying magnetization dynamic of magnetic films and nanostructures.[1–4] A thin ferromagnetic film is placed close to the surface of CPW upside down so that a substrate is the furthest outer medium from the CPW. A microwave field $\tilde{h}$ proportional to the rf current in the central CPW line excites the precession of the magnetization $\tilde{m}$, which in turn induces a microwave voltage in CPW. The FMR response is commonly extracted from the reflection (S_{11}) or transmission (S_{21}) coefficients of scattering parameters using VNA and, hence, the technique is referred to as VNA-FMR[3] or broadband FMR.[5] In practice, only the changes of S_{21} (or S_{11}) due to FMR absorption are of interest and they are detected in frequency swept mode[2] with the magnetic field kept fixed or in the field-swept mode at a chosen frequency while sweeping the field.[4] The latter mode is more convenient. It has been proved that a change ΔS_{12} (or ΔS_{11}) due to microwave absorption of a single ferromagnetic film is proportional to the imaginary part of complex susceptibility $\chi^{''}$,[1,6,7] so that ΔS_{12} vs. H reflects the Lorentzian curve characteristic of FMR absorption.

However, in the case of thin film structures containing normal metals conducting cap/buffer layer interpretation of the experimental results of VNA-FMR experiments with a CPW is complicated.[1] In opposite to the standard FMR experiments based on microwave cavities with the microwave field of a substantial homogeneity, in CPW the microwave field is asymmetric with regard of a magnetic thin film and inhomogeneous due to shielding of microwave fields by the eddy currents flowing along the conducting films.[5,8] As a result, higher order spin wave modes are relatively easily excited with the use of a CPW set-up resulting in the spin wave resonance (SWR).[9] In a series of papers[5,10] the effect of conductivity of planar ferromagnetic structures on a FMR (SWR) response has been examined. It has been found experimentally[5] that CPW efficiently excites higher order standing spin waves across the film thickness of 30-90 nm. The ratio of SWR mode amplitudes strongly depends on ordering of layers. All experimental data has been found to be consistent with the expected effects of eddy currents in the conducting thin film structures with thickness below the microwave skin depth. A strong asymmetry in the FMR response of a bilayer magnetic film has been studied theoretically.[10] The response has been found also to depend on ordering of FM layers with respect to a microstrip transducer. This effect has been explained as shielding by eddy currents induced in thin film structures which remain efficient even for nm thick films. More recently, it has been shown[11] that a nonmagnetic capping/seed layers forming an external shielding protection decrease the nonuniformity of the magnetic field inside a magnetic thin film structure. Specifically, when a plane wave is reflected from a metallic film thinner than the skin depth, the electric field $\tilde{e}$ is reflected from the film surface close to a CPW, whereas the magnetic field $\tilde{h}$ penetrates into the FM film and is reflected from the outer surface of the stack. Consequently, by adding a highly conducting Cu (Au) layer, an increase of reflection from the FM film is expected.

Recently, Bailleul[12] has shown that the propagation of microwave fields along CPW is strongly modified when a nonmagnetic, normal metal such as Au or Cu film is brought close to it. This shielding effect is expected to have important consequences for a broadband FMR ex-

periments. In particular, the shielding of the magnetic $\tilde{h}$ and/or the electric microwave field $\tilde{e}$ results in a strong modification of the characteristic impedance Z_c and the propagation index. Important is that once shielded, the electric and magnetic fields are concentrated in the air gap separating the CPW and the conducting nonmagnetic metal film.

Thicknesses of ferromagnetic layers discussed in the above papers were of 30-90 nm enabling excitations of higher order SWR modes. The present paper represents an experimental extension of the above papers to ultrathin ferromagnetic layers for which macrospin model[13] is regarded to be fully fulfilled. In ultrathin ferromagnetic films only the fundamental mode is excited with no spatial variation of the magnetization across the film thickness.[13] The purpose of the paper is to investigate the effect of a nonmagnetic buffer layer on the FMR response of either a single ultrathin Co films or multilayer structures comprising ultrathin exchange decoupled ferromagnetic layers. In particular, we will be interested in answering how the FMR absorption amplitude (or area under absorption curve) depends on the thickness of the buffer layer.

II. EXPERIMENTAL DETAILS

The multilayer thin films investigated in the present paper by using VNA-FMR are intended for spin-transfer oscillators[14] that comprise a [Au/Co]×4 perpendicular polarizer, an in-plane magnetized [Py/Co] free layer with Permalloy (Py), and an in-plane Co analyzer in contact with IrMn antiferromagnetic layer. Additionally, two multilayers [Au-wedged/Co/Au] were also investigated as the reference samples. The composition of the multilayers with the thickness of individual layers in nanometers are shown in Tab. I. The continuous multilayer films were deposited in a Prevac sputtering system onto high resistivity ($\rho > 2$ kΩ cm) Si/SiO_2 substrates that contain an Ti/Au buffer layers of various thickness. The base pressure was less than 1×10^{-6} Pa and the Ar pressure was approximately 10^{-2} Pa. All structures were covered with a 5 nm Au cap layer. For VNA-FMR investigations, the films on the substrates of 19 × 15 mm were cut to approximately 10 × 15 mm samples. The total thickness of the structures investigated (30-100 nm) including conducting buffer layer is well below the skin depth of the electromagnetic field of 20 - 30 GHz. Additionally, two reference samples consisting of ultrathin 2.5 nm Co on Ti 4nm/Au wedge buffers 10 - 40 nm and 30 - 60 nm, respectively, were deposited at the same conditions.

Crystalline structure was determined using X-ray diffraction. Diffraction profiles were measured in the Bragg-Brentano geometry and analysis of the diffraction profiles indicates that the Au buffers show a strong (111) texture since only the (111) and (222) peaks were visible. The width of diffraction lines are 0.7 deg, 1 deg, for the free Py/Co layer and IrMn, respectively. For a 10 and 40 nm thick Au buffer, the width is 1.1 deg and 0.4 deg, respectively. Using the Scherrer formula we estimate the crystallite size as 9, 25 nm for the 10 and 40 nm Au buffer, respectively. On the basis of fitting procedure with the use of SimulReflec[15] software of x-ray reflectivity data the composition profiles of a few chosen multilayers were determined as it is shown in Fig. 1 for the sample SC as a typical example. As it is seen in the inset in Fig. 1, thicknesses of the individual layers making up the buffer, free layer and analyzer are in agreement with those determined from technological parameters. The roughness estimated from the fitting is of 0.5 - 0.7 nm. Magnetization reversals of the multilayers were examined using a standard vibrating sample magnetometer at room temperature. The measurements confirmed that the multilayers comprise the perpendicular magnetized polarizer (with the perpendicular anisotropy field of 15 - 19 kOe), the in-plane magnetized free layer, and the analyzer with exchange-bias field of 200 Oe.

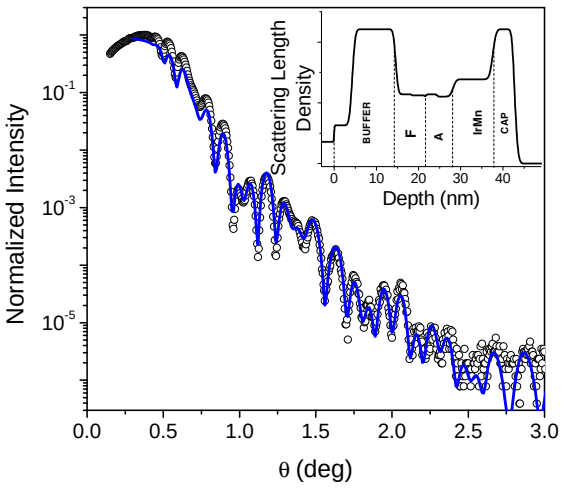

FIG. 1. X-ray reflectivity of the multilayer sample SC. The model calculation was performed with the same parameters as presented in Tab. I and interface roughness of 0.5 - 0.7 nm. The composition profile of the whole structure is shown in the inset

III. CPW VNA-FMR MEASUREMENT TECHNIQUE

A broadband FMR spectrometer based on VNA-FMR technique was used to measure the FMR spectra of multilayers in the in-plane geometry with an external magnetic field applied in the sample plane. An in-plane microwave field with a frequency of 20 - 30 GHz was applied to the sample using a grounded CPW with a 0.45 mm wide central strip. Our CPW design is similar to that of Southwest Microwave Inc.[16] The samples (10 × 15 mm) were placed face down on the waveguide so that the buffer layer was always the furthest layer in the investigated multilayer structures. The complex transmission parameter S_{21} was measured with a VNA at a fixed frequency

TABLE I. Composition of multilayer structures comprising polarizer (P), analyzer (A), and free layer (F) separated in between with Cu spacers. All samples are covered with a Au 5 nm cap layer. Polarizer consists of Au/Co bilayers repeated four times. Reference samples comprise only a buffer layer, a free Co layer, and a cap layer.

sample	buffer	sequence of P, A, F layers		
		P	**F**	**A**
SA[a]	Ti 4/Au 40	(Au 1/**Co** 0.7)$_4$	Cu 4/**Py** 3/**Co** 0.5	Cu 3/**Co** 3/IrMn 15
		A	**F**	**P**
SB	Ti 4/Au 40	IrMn 10/**Co** 3	Cu 3/**Co** 0.5/**Py** 3	Cu 4/(Au 1/**Co** 0.7)$_4$ [b]
			F	**A**
SC	Ti 4/Au 10	-	Cu 3/**Co** 0.5/**Py** 3	Cu 4/**Co** 3/IrMn 10
		A	**F**	**P**
SD	Ti 4/Au 10	IrMn 10/**Co** 3	Cu 3/**Co** 0.5/**Py** 3	Cu 4/(Au 1/**Co** 0.7)$_4$
Ref-1	Ti4/Au wedge(10-40)	-	**Co** 2.5	Au 5-cap
Ref-2	Ti4/Au wedge(30-60)	-	**Co** 2.5	Au 5-cap

[a] Samples SA1 and SA2 have the same structure except buffer layers: $(Ti2/Au2)_5$ for SA1 and $(Ti2/Au2)_{10}$ for SA2.
[b] The subscripts denote the number of repetition and the other numbers denote thickness in nanometers.

- typically 20 GHz - while the external magnetic field was swept between +10, 0, and -10 kOe. Since FMR signals were measured in two quadrants, the number FMR peaks is doubled as it is shown in Fig. 2. We find such a measurement procedure helpful in estimating errors in calculations of the area under absorption curve. Figure 2 (a) shows typical real part Re S_{21} and imaginary part Im S_{21} of a complex scattering factor $S_{21} \times exp(i\phi)$ with a phase ϕ correction.[17] Two main features characterize Im S_{21} vs. H: a quasi-parabolic background Im S_{21}^0 which is related to a nonresonant background of the whole microwave track and six characteristic absorption peaks (three for positive and three for negative H, respectively) plus one central peak. The tree peaks P^+, F^+, and A^+ (or, P^-, F^-, and A^-, for negative field direction) are related to FMR absorption of the exchange decoupled polarizer, free layer, and analyzer, respectively. The central peak, which is centered at $H = 0$ Oe, is slightly asymmetric due to unidirectional anisotropy of the analyzer. The central peak is related to a additional absorption during magnetization reversal of the F+A structure. The central peak will not be discussed further in this paper and it will be a subject of future paper.

Figure 2 (a) clearly shows that the experimental data of Im S_{21} can be broken into magnetic and nonmagnetic contributions assuming that a reflection of microwave power is weak in our VNA-FMR set-up. Therefore, following a similar analysis discussed in Refs. 6 and 7, the complex S_{21} scattering term may be expressed as

$$S_{21}(H,t) \approx S_{21}^0(H,t) + \frac{\chi(H)}{\chi_0}, \qquad (1)$$

where $\chi(H)$ is complex microwave susceptibility, χ_0 is complex function of the experimental parameters , such as frequency and film thickness[7]. Furthermore, time t takes into account some drift of S_{21}^0 during measurements. Assuming that $S_{21}^0(H,t)$ depends on H in a nonresonant way and also depends on t, we can reasonably approximate $S_{21}^0(H,t) \approx AH + BH^2$ so that we arrive at a simple relation

$$\chi(H) \approx \chi_0 \Delta S_{21}(H), \qquad (2)$$

where Δ S_{21} =S_{21}-S_{21}^0. Figure 2 (b) shows the measured Im $\Delta S_{21}(H)$) after subtraction of the nonresonant background Im $S_{21}^0(H)$. It can be easily shown that the experimental spectrum can be deconvoluted using a set of Lorentzians. Slight differences in the height and linewidth ΔH (FWHM) for P^+, P^- and F^+,F^- peaks serve here as a rough estimate of uncertainties in determination of ΔS_{21} absorptions in our VNA-FMR set-up. Keeping in mind that $\chi^{''} \approx \chi_0\, Im\, \Delta S_{21}(H)$, we can further express the area under FMR absorption peak I as

$$I \propto \int \chi^{''} dH. \qquad (3)$$

In theory, the intensity of FMR signal I measured in a microwave cavity is proportional the total magnetic moment.[18] However, in this case FMR intensity studies require a microwave system which can provide reproducible results with a special emphasis on the microwave cavity coupling and cavity quality factor.[19] In contrary to the discussion in Ref. 4, we found the magnitude of the FMR absorption ($\propto$ Im ΔS_{21}) quite stable for the structures of the same size and the same composition. It suggests that we can compare the intensities of FMR absorption of various samples provided that the measurement conditions in a CPW set-up are the same. In section IV, we will provide the experimental evidence that VNA-FMR can be used not only for quantitative determination of the resonance field H_r and the resonance linewidth ΔH but also for comparative measurements of the microwave power absorbed by ultrathin films of the same geometry and we will show how a specific ordering in a stack of magnetic and nonmagnetic ultrathin layers affects the microwave absorption.

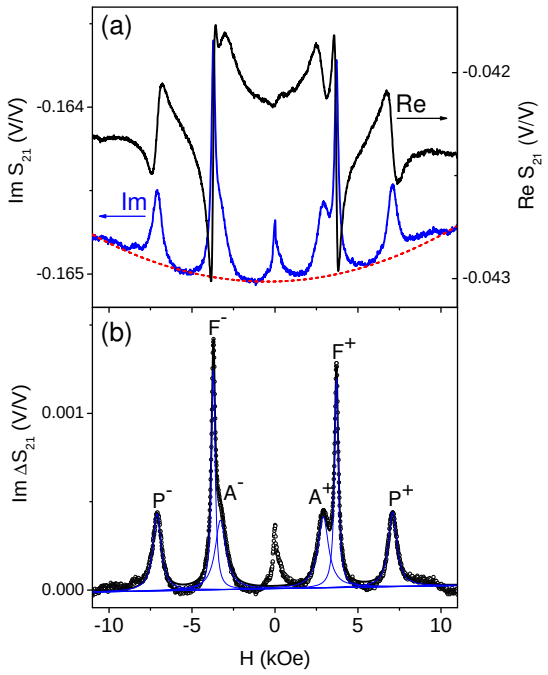

FIG. 2. (a) Typical in-plane VNA-FMR spectrum of sample SA with the real Re S_{21} and imaginary Im S_{21} parts of complex transmission parameter S_{21}. (b) The same spectrum with the values of Im ΔS_{21} adjusted by removing the background and the linear drift. The spectrum was measured with the magnetic field sweep from + 10 kOe to -10 kOe so that the number FMR absorptions is doubled. The central peak at $H = 0$ is related to an absorption due to magnetization reversal. Blue lines (in colors - online) show the fits of the spectra with the Lorentzians.

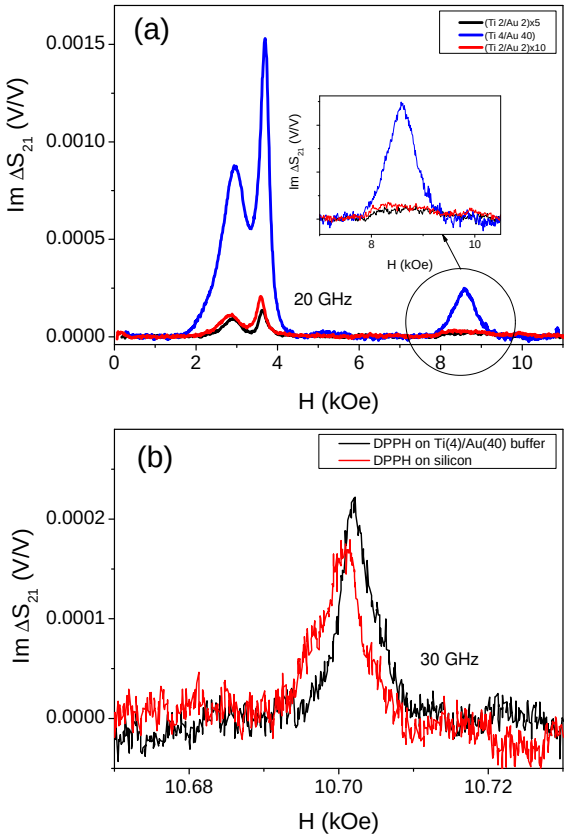

FIG. 3. (a) Comparison of FMR absorption in three magnetic structure (SA, SA1, and SA2) in contact with buffer layers of various structure/sheet resistance. (b) Comparison of EPR signal from a DPPH film on a 40 nm Au buffer and on bare Si substrate.

IV. VNA-FMR RESULTS

We prepared three thin film structures comprising identical P, F, and A on three different buffer layers: Ti 4/Au 40 (SA), (Ti 2/Au 2)×5 (SA1), and (Ti 2/Au 2)×10 (SA2) (see Tab. I, for details). In spite of the fact that the structures had nearly the same magnetic properties (e.a., the same resonance fields of A, F, and P and similar magnetic moments) the signal amplitude of Im ΔS_{21} was found to be the highest for sample SA as it is shown in Fig. 3 (a). While the positions of FMR responses for SA, SA1, and SA2 (dashed lines in Fig. 3 (a)) are nearly the same for A, F, and P, respectively, the signals from the sample SA with the thickest Au buffer layer is nearly 6 - 7 times higher than those of samples SA1 and SA2. The effect of signal enhancement is even more pronounced for the polarizer P with perpendicular anisotropy (see the inset in Fig. 3 (a)). While the FMR absorptions for samples SA1 and SA2 are barely seen from the noise, the FMR absorption of P in SA is substantial and comparable with those of A and F. As it was shown in our recent paper,[20] the enhancement in this case is presumably additionally influenced by a better texture and crystallite size of the polarizer, which was grown on the thick Au 40 buffer layer.

Therefore, Fig. 3 (a) can be regarded as an experimental evidence of shielding of the electromagnetic field in a CPW by a conducting film with a low sheet resistance. It shows that a highly conducting buffer layer that is the outer conducting layer from CPW can beneficiary affect the excitation of the fundamental mode(s) in our ultrathin film structure. We checked using a four-point probe that the sheet resistance of SA, SA2, and SA1 buffer layers is of 0.5, 15 and 30 Ω, respectively. Such a change in the sheet resistance has recently been shown to strongly affect shielding of either $\tilde{h}$ or $\tilde{e}$ fields.[12] To check if the field $\tilde{h}$ is really enhanced due to a conducting film alone, we performed a similar experiment using DPPH - common EPR standard compound - dissolved in a nonconducting glue and then deposited on bare Si substrate and on Si substrate covered with Ti 4/Au 40 buffer layer, respectively. No such enhancement due to Au buffer layer

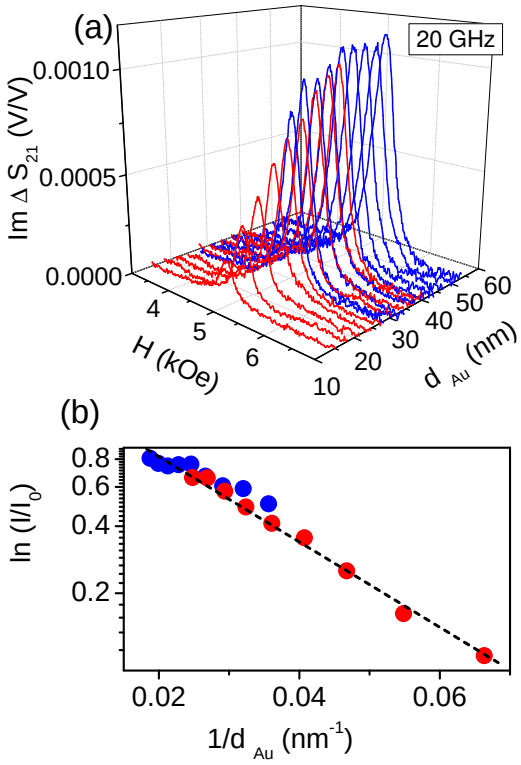

FIG. 4. (a) 3-D plot of FMR absorption of a 2.5nm Co film deposited onto Ti 4/Au (10 - 40) (red - sample Ref-1) and Ti 4/Au (30 - 60) wedge (blue - sample Ref-2) , respectively. (b) Log-lin dependence of the normalized FMR intensity I/I_0 on the inverse thickness of Au buffer layer.

was observed as it is shown in Fig. 3 (b). We argue that the lack of any enhancement in the absorption amplitude results from insulating nature of DPPH "layers". Hence, the effect is attributed to the conducting FM films in the immediate proximity of conducting nonmagnetic layers.

To determine the relation between the amplitude of FMR absorption (Im ΔS_{21}) and the thickness of buffer layer, we measured FMR absorption in a single ultrathin 2.5 nm Co layer buried between a buffer Au layer of various thickness and a 5 nm Au cap layer. The measurements were carried on two reference samples (Tab.I) with the buffer layer deposited in a wedge shape from 10-40 nm and from 30-60 nm, respectively. The results of FMR measurements are shown in Fig. 4 (a) as a 3-D plot. It is clearly seen that the amplitude of FMR absorption of the buried Co 2.5 nm layer increases with the thickness of the Au buffer layer and saturates at its thickness of 40-60 nm. Since the linewidth (defined as the width of the FMR absorption at half hight) also increases with the thickness of the buffer Au layer from 340 Oe to 440 Oe, we find that the intensity of FMR absorption (e.a., the area under absorption curve) is the best characteristic of the microwave absorption. It appears that the dependence of the intensity I vs. $1/d_{Au}$ (see Fig. 4 (b)) can be approximated by the following expression:

$$I = I_0\ exp\ (-\frac{d_o}{d_{Au}}) = I_0\ exp\ (-\frac{R_{sr}}{R^o_{sr}}), \qquad (4)$$

where d_o is of 38 nm and I_0 is of 1.7. The sheet resistance of a thin Au buffer layer is defined as $R_{sr} = \rho/d_{Au}$. If we take the resistivity of bulk gold as 3 $\mu\Omega$cm, R_{sr} of the Au buffer varies from 2 Ω to 0.33 Ω for the Au thickness of 10 and 60 nm, respectively. Fitting to the experimental data using Eq. (4) gives R^o_{sr} of 0.8 Ω. It is worth noticing that the resonance field H_r also experiences a small change with the thickness of the Au buffer layer (not shown). The reason might be a joint effect of a small increase in the perpendicular anisotropy due to increase of crystallite sizes for thicker Au buffer layer and a small frequency shift due to inhomogeneous excitation of microwave fields[1]. However, this subject is out of scope of the present paper. To sum up, we show for two ultrathin Co films that the Au buffer thickness (e.a., its sheet resistance) has a strong impact on the intensity of FMR absorption measured using CPW. It changes in a regular way expressed by Eq. (4).

To further confirm the enhancement of FMR absorption, we compared the FMR absorption spectra of four SA-SD structures deposited either on the Ti 4/Au 40 (the samples SA and SB) or Ti 4/Au 10 buffers (the samples SC and SD). The FMR absorption spectra are shown in Fig. 5. As can be seen in Tab. I and in the insets in Fig. 5, the samples differ in the sequences of the magnetic layers P, F, and A. The P-F-A and A-F-P structures are referred to as a simple and an inverse structure, respectively. For some purposes, which are out of scope of the present paper, the sample SC has no polarizer. Comparing Figs. 5 (SA),(SB) with (SC), and (SD), one can see that the FMR amplitudes for the samples SA and SB deposited on the the Ti 4/Au 40 are about ten times higher than those of the samples SC and SD deposited onto the Ti 4/Au 10 buffer. Besides, a clear decrease in signal to noise ratio is seen in Fig. 5 for SA and SB in comparison with SC and SD structures. It confirms again the previous results shown in Figs. 3 (a) and 4 (a).

In FMR theory with ellipticity of precession included[19], a ratio of the intensities I of P, F, and A should scale with their magnetic moments that are comparable in fact (e.a., $m_P : m_F : m_A \approx 1.0 : 0.8 : 1.07$). It is true, to same extent, in the case of P and F layers. However, in the case of analyzer A with the IrMn layer in close contact with the Au buffer (SB and SD) the absorption intensity is strongly diminished.

V. DISCUSSION

Discussion of our experimental data is grounded on the core results of Ref. 10. (i) In contrast to the common cavity FMR measurements, a conducting thin film sample in CPW - FMR is illuminated by microwaves asymmetrically from the front surface of the film as it is shown in

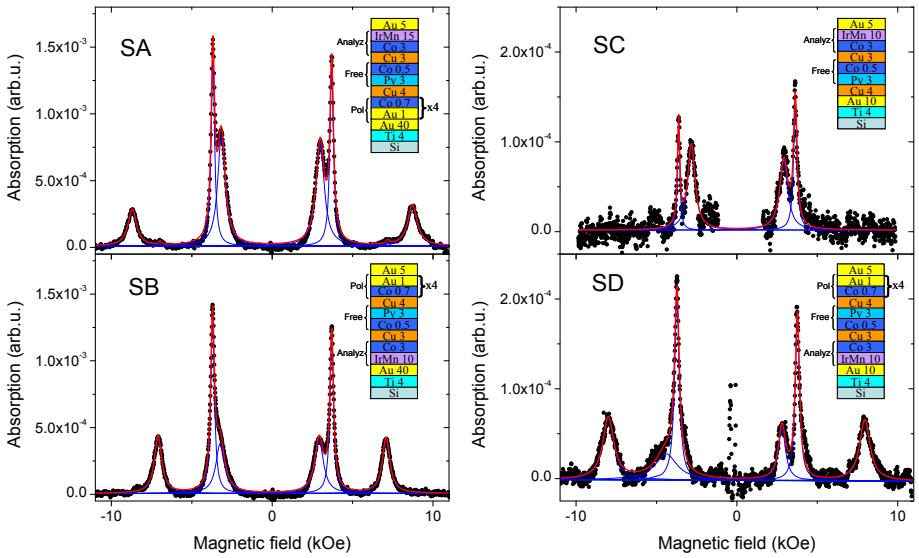

FIG. 5. FMR absorption vs. H of a series of SA - SD multilayer thin film structures prepared for spin-transfer-torque oscillators with a perpendicular polarizer P, a free layer F, and an in-plane analyzer A pinned to IrMn layer. Blue lines (in colors - online) show the fits of the spectra with the Lorentzians. The "central"peak is subtracted for clarity.

Fig. 6. (*ii*) In such a geometry, the thin film sample with a thickness d less than the skin depth $\delta_S = \sqrt{2/\mu_0\sigma\omega}$ the microwave magnetic field decays more strongly than exponentially. (*iii*) In a highly conducting film the microwave magnetic field is strongly inhomogeneous.

Based on the multireflection model, we can write the scattering parameter S_{21} of the scattering matrix in terms of the complex reflection coefficient Γ and the complex propagation factor $\gamma_0\gamma_f$. The complex propagation factor of the unloaded CPW $\gamma_0 = i\omega/\upsilon_{ph}$, where ω is the angular frequency of microwave field and υ_{ph} is the phase velocity of microwaves in CPW.[3] γ_f is the propagation index of the loaded CPW:

$$\frac{S_{21}}{S_{21}^0} = \frac{\Gamma^2 - 1}{\Gamma^2 \exp(-\gamma_0\gamma_f\delta) - \exp(\gamma_0\gamma_f\delta)}, \qquad (5)$$

where δ is the film width and S_{21}^0 is the scattering parameter of the empty CPW. Keeping only linear term in expansion of Eq. (5) and assuming $|\Gamma| \ll 1$,[5] we obtain

$$\frac{S_{21}}{S_{21}^0} = \exp(-\gamma_0\gamma_f\delta). \qquad (6)$$

The propagation index γ_f can be further approximated in terms of characteristic impedance $\gamma_f = \sqrt{\frac{Z_0 - Z_r}{Z0}} \approx 1 + \frac{Z_r}{2Z_0}$, (Eq. (13) in Ref. 10), where Z_0 is characteristic impedance of the unloaded CPW and Z_r is the surface impedance of the thin film placed on CPW. Hence,

$$\frac{S_{21}}{S_{21}^0} = \exp\left(-\gamma_0 \frac{Z_r}{2Z_0}\delta\right). \qquad (7)$$

According to the discussion of Bailleul[12]

$$Z_r = R_{sr}\frac{\delta}{w} = \frac{\rho}{d}\frac{\delta}{w}, \qquad (8)$$

where R_{sr} is the sheet resistance of the film with the resistivity ρ, thickness d, and w is the width of the central line of CPW (see. Fig. 2 in Ref. 12). Eventually, in accordance with Ref. 10, we can express the measured scattering coefficient S_{21} in terms of geometrical parameters of CPW and the film placed on it

$$\frac{S_{21}}{S_{21}^0} \propto \exp\left(-\frac{\frac{\gamma_0\rho\delta^2}{2Z_0 w}}{d}\right) \propto \exp\left(-\frac{d_0}{d}\right), \qquad (9)$$

which has the same form as the fitting formula Eq. (4) to the experimental data shown in Fig. 4. Let us estimate d_0. For $Z_0 = 25 - 50\ \Omega$, $|\gamma_0| = \omega/\upsilon_{ph} = 7\ \mathrm{cm}^{-1}$, $\delta = 0.4$ cm, $\upsilon_{ph} = 1.8 \times 10^{10}$ cm/s, and $\omega/2\pi = 20$ GHz the estimated range of d_0 is between 8 and 15 nm if we assume the resistivity $\rho = 3\ \mu\Omega$cm of the gold buffer the same as for bulk. In practice, the resistivity of several nanometers thick gold films is several times higher[21] so that $d_o = 38$ nm estimated from fitting of the experimental data (Fig. 4) according to Eq. (4) is in agreement with the above model. Since in a number of spintronic devices and magnonic structures coplanar waveguides (microantennas) are widely used, the observed FMR signal enhancement may be useful for applications.[22]

Let us assume that an ultrathin Co 2.5 nm film is deposited on a gold wedged buffer layer of thickness $10 < d < 50$ nm as shown in Fig. 6. The Co film is very thin in comparison to the Au buffer layer so it actually plays the role of a tag useful for monitoring the dynamic magnetic field. Since it is very thin, we assume the entire structure as a nonmagnetic with conductivity of gold wedge (region 2). Transverse wave with wavenumber k_1 and with the amplitude equal unity is incident perpendicular to the film surface from region 1 with the permittivity ϵ_1 the same as for region 3.[10] The permittivity

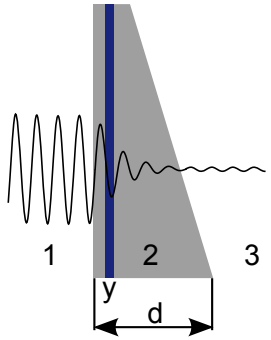

FIG. 6. A sketch showing an ultrathin Co 2.5 nm film on a Au buffer layer so that the entire structure forms a wedge $10 < d < 50$ nm thick. Microwaves are partially reflected and transmitted through the wedge.

of region 2 ϵ_2 is complex. Taking continuity boundary conditions at the boundaries of regions 1, 2, and 3 for $\tilde{h}_x$ and $\tilde{e}_z$ we have

$$\tilde{h}_{x\,1} = \exp(-ik_1 y) + B_1 \exp(ik_1 y), \tag{10}$$

$$\tilde{h}_{x\,2} = A_2 \exp(-ik_1 y) + B_2 \exp(ik_1 y), \tag{11}$$

$$\tilde{h}_{x\,3} = A_3 \exp(-ik_1 y) \tag{12}$$

with

$$B_1 = \frac{(r-1)\exp(2ik_2 d) - 1}{D}, \tag{13}$$

$$A_2 = \frac{2(1+\sqrt{r})\exp(2ik_2 d) - 1}{D}, \tag{14}$$

$$B_2 = \frac{2(\sqrt{r}-1)}{D}, \tag{15}$$

$$A_3 = \frac{4\sqrt{r}\exp[ik_2(1+\sqrt{r})d]}{D}, \tag{16}$$

where $r = \epsilon_1/\epsilon_2$ and $D = \exp(2ik_2 d)(1+\sqrt{r})^2 - (1-\sqrt{r})^2$. Since $\epsilon_1 = 1$ and ϵ_2 of gold is imaginary and very large,[5] $\mid r \mid \ll 1$ so that after expanding exponential functions and keeping only the linear terms of expansions we obtain that $\tilde{h}$ varies linearly with y as

$$\tilde{h}_{x\,2} \approx 2\frac{d-y}{d}, \tag{17}$$

where 2 denotes that the amplitude at the front of the structure is doubled due to positive interference.

In order to extend the model of inhomogeneous dynamic magnetic field within a more complicated structure comprising P+F+A layers and a Au buffer layer, let us compare the FMR intensity of the CPW-FMR responses shown in Fig. 5. In contrast to a single ultrathin Co film on the Ag buffer layer, the P+F+A ferromagnetic structure is more extended (of ~ 20 nm) and consists of exchange decoupled (the Cu spacers are 3 - 4 nm thick) Co and Permalloy layers with diverse effective anisotropies. This makes possible observation of well separated FMR absorptions of each layer. Exact calculations of electromagnetic field distribution in such structures would need a set of many boundary conditions[11] with several material parameters. However, we make use of Eq. (17) taking into account that $\tilde{h}$ in the multilayer is a linear combination of $\tilde{h}$ in individual layers and its slope scales with a sheet resistance (ρ/d) of the individual layers.[5] Hence, the lower R_{rs} the higher is the slope of $\tilde{h}$ within a layer. R_{rs} values of the individual layers in the entire stack are quite diverse - R_{rs} is the highest for IrMn layer[23] and the lowest for Au buffers. Possible distributions of the dynamic field $\tilde{h}$ (black lines) are shown in Fig. 7 (a), (b), and (c) for SA, SB, and SD structures, respectively. In other words, we assume in accordance with Eq. (17) that $\tilde{h}(0) = 2$ and $\tilde{h}(d) = 0$ what is generally not true for very thin stacks (see Fig. 6 in Ref. 10) so that the microwaves can be partially transmitted out of the stack as it is shown in Fig. 7 (c). Nonetheless, the distributions of $\tilde{h}$ just depict graphically that its slope in the P+F+A stacks is the highest for the SD sample and the lowest for the SA sample so that the magnetic field inside the SA sample is the most homogeneous. It is also seen that the position of antiferromagnetic IrMn pinning layer plays an important role in the distribution of $\tilde{h}$ because its resistivity[23] is about 100 times higher than that of Au.[21] As it is shown in Tab. II, the ratio of the magnetic moments of

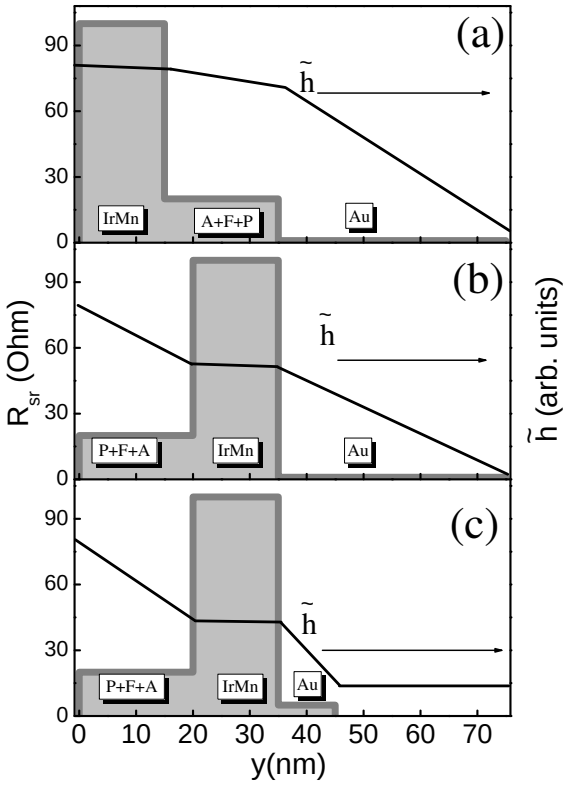

FIG. 7. Distribution of the dynamic magnetic field $\tilde{h}$ inside SA (a), SB (b), and SD (b) structures with diverse sheet resistance R_{rs} of individual layers.

TABLE II. Ratios of magnetic moments and FMR intensities of P, F, and A layers in SA, SB, and SD structures.

Sample	m_P	m_F	m_A
SA,SB,SD	1	0.8	1.07
	I_P	I_F	I_A
SA	1	0.84	0.97
SB	1	0.86	0.58
SD	1	0.64	0.40

P, F, and A layers is $m_P : m_F : m_A = 1 : 0.8 : 1.07$ one would expect the same ratio for the intensity of FMR absorption of P, F, and A, respectively if the dynamic field $\tilde{h}$ is homogeneous. Clearly, this is not the case since the measured ratios $1 : 0.86 : 0.58$ and $1 : 0.64 : 0.4$ for the sample SB and SD, respectively. Hence, in accordance with the sketch in Fig. 7, the dynamic magnetic field is the most inhomogeneous SD structure. On the contrary, for SA structure the ratio is in a fairly good agreement with the ratio of magnetic moments estimated from geometry for P+F+A layers.

VI. CONCLUSIONS

In the present paper, we have extended previous broadband FMR studies of thin magnetic films[1–10] to ultrathin magnetic film structures deposited on the buffer layers with diverse sheet resistance R_{sr}. We have shown that the intensity of FMR absorption in the single ultrathin Co layer measured with the use of coplanar waveguide (CPW) depends on the thickness d of the conducting Au buffer $\propto \exp(-1/d)$ or, equivalently, on the buffer sheet resistance $\propto \exp(-R_{sr})$. We have also shown that the measured in CPW VNA-FMR absorption intensity of the systems composed of several exchange decoupled ultrathin magnetic layers do not scale in proportion to their magnetic moments as could be expected. On the contrary, the intensity of FMR absorption ratios of the individual ultrathin layers depend on their ordering with respect of CPW, which plays the role of both a transmitter and a receiver of microwaves. The above mentioned findings are interpreted in terms of the microwave shielding effect by conducting films and an inhomogeneity of the dynamic magnetic field $\tilde{h}$ related to the shielding.

ACKNOWLEDGMENT

This work was supported by the Polish-Swiss Research Program NANOSPIN PSRP-045/2010.

[1] G. Counil, P. Crozat, T. Devolder, C. Chappert, S. Zoll, and R. Fournel, IEEE Trans. Magnetics **42**, 3321 (2006).
[2] I. Neudecker, G. Woltersdorf, B. Heinrich, T. Okuno, G. Gubbiotti, and C. Back, J. Magn. Magn. Mater. **307**, 148 (2006).
[3] C. Bilzer, T. Devolder, P. Crozat, C. Chappert, S. Cardoso, and P. Freitas, J. Appl. Phys. **101**, 074505 (2007).
[4] I. Harward, T. O'Keevan, A. Hutchison, V. Zagorodnii, and Z. Celinski, Rev. Sci. Instr. **82**, 095115 (2011).
[5] K. J. Kennewell, M. Kostylev, N. Ross, R. Magaraggia, R. L. Stamps, M. Ali, A. A. Stashkevich, D. Greig, and B. J. Hickey, J. Appl. Phys. **108**, 073917 (2010).
[6] H. T. Nembach, T. J. Silva, J. M. Shaw, M. L. Schneider, M. J. Carey, S. Maat, and J. R. Childress, Phys. Rev. B **84**, 054424 (2011).
[7] Y. Ding, T. Klemmer, and T. Crawford, J. Appl. Phys. **96**, 2969 (2004).
[8] K. J. Kennewell, M. Kostylev, and R. L. Stamps, J. Appl. Phys. **101**, 09D107 (2007).
[9] D. C. Crew, K. J. Kennewell, M. J. Lwin, R. C. Woodward, S. Prasad, and R. L. Stamps, J. Appl. Phys. **97**, 10A707 (2005).
[10] M. Kostylev, J. Appl. Phys. **106**, 043903 (2009).
[11] I. S. Maksymov and M. Kostylev, J. Appl. Phys. **113**, 043927 (2013).
[12] M. Bailleul, Appl. Phys. Lett. **103**, 192405 (2013).
[13] B. Heinrich and J. C. Bland, *Ultrathin Magnetic Structures II* (Springer Berlin Heidelberg, 2005) pp. 195–296.
[14] D. Houssameddine, U. Ebels, B. Delaët, B. Rodmacq, I. Firastrau, F. Ponthenier, M. Brunet, C. Thirion, J.-P. Michel, L. Prejbeanu-Buda, *et al.*, Nature materials **6**, 447 (2007).
[15] SimulReflec, "Lab. Leon Brillouin CEA/CNRS UMR12," (2007), http://www-llb.cea.fr/prism/programs/simulreflec/simulreflec.
[16] B. Rosas, "The Design and Test of Broadband Launches up to 50 GHz on Thin and Thick Substrates," (2011), http://mpd.southwestmicrowave.com/resources/.
[17] S. S. Kalarickal, P. Krivosik, M. Wu, C. E. Patton, M. L. Schneider, P. Kabos, T. J. Silva, and J. P. Nibarger, J. Appl. Phys. **99**, 093909 (2006).
[18] A. Gurevich and G. Melkov, *Magnetization Oscillations and Waves* (CRC Press, 1996).
[19] Z. Celinski, K. Urquhart, and B. Heinrich, J. Magn. Magn. Mater. **166**, 6 (1997).
[20] M. Matczak, B. Szymański, M. Urbaniak, M. Nowicki, H. Głowiński, P. Kuświk, M. Schmidt, J. Aleksiejew, J. Dubowik, and F. Stobiecki, J. Appl. Phs. **114**, 093911 (2013).
[21] J. R. Sambles, K. C. Elsom, and D. J. Jarvis, Phil. Trans. of the Royal Soc. of London A **304**, 365 (1982).
[22] V. V. Kruglyak, S. O. Demokritov, and D. Grundler, J. Appl. Phys. **115**, 043917 (2014).
[23] R. Y. Umetsu, K. Fukamichi, and A. Sakuma, Mater. Trans. **47**, 2 (2006).